THE JOURNAL OF BIOLOGICAL CHEMISTRY
Vol. 279, No. 24, Issue of June 11, pp. 25567–25573, 2004

Printed in U.S.A.

The Inner Nuclear Membrane Protein Lamin B Receptor Forms Distinct Microdomains and Links Epigenetically Marked Chromatin to the Nuclear Envelope*

Received for publication, December 12, 2003, and in revised form, March 25, 2004
Published, JBC Papers in Press, March 31, 2004, DOI 10.1074/jbc.M313606200

Dimitra Makatsori‡§, Niki Kourmouli¶, Hara Polioudaki‖, Leonard D. Shultz, Kelvin Mclean‡‡, Panayiotis A. Theodoropoulos‖, Prim B. Singh¶, and Spyros D. Georgatos‡§§**

*From the ‡Laboratory of Biology, The University of Ioannina, School of Medicine, 45 110 Ioannina, Greece, the ¶Nuclear Reprogramming Laboratory, Department of Gene Expression and Development, The Roslin Institute, EH25 9PS Edinburgh, Scotland, United Kingdom, the ‖Department of Basic Sciences, The University of Crete, School of Medicine, 95 110 Heraklion, Crete, Greece, the **Jackson Laboratory, Bar Harbor, Maine 04609, and the ‡‡Functional Genomics Unit, The Moredun Research Institute, EH26 0PZ Penicuik, Midlothian, Scotland, United Kingdom*

Using heterochromatin-enriched fractions, we have detected specific binding of mononucleosomes to the N-terminal domain of the inner nuclear membrane protein lamin B receptor. Mass spectrometric analysis reveals that LBR-associated particles contain complex patterns of methylated/acetylated histones and are devoid of "euchromatic" epigenetic marks. LBR binds heterochromatin as a higher oligomer and forms distinct nuclear envelope microdomains *in vivo*. The organization of these membrane assemblies is affected significantly in heterozygous *ic* (ichthyosis) mutants, resulting in a variety of structural abnormalities and nuclear defects.

A significant proportion of heterochromatin is localized in the periphery of the cell nucleus and maintains a close spatial association with the inner nuclear membrane (1–5). This spatial association reflects a multiplicity of interactions between chromatin components and integral or peripheral proteins of the nuclear envelope (NE)[1] (6, 7).

Because chromatin is extensively and differentially modified (8, 9), it is tempting to think that certain epigenetic marks or factors associated with histone modifying enzymes provide binding sites for NE proteins. However, it is equally possible that transcriptionally active, noncondensed chromatin is subjected to silencing and "heterochromatinization" upon contact to the NE. Both of these hypotheses receive experimental support: chromatin that is silenced through binding to SIRs can tether itself to the NE (10), whereas targeting of marker genes to the inner nuclear membrane suppresses their expression (11).

One of the factors that have been implicated in chromatin anchorage to the NE is the lamin B receptor (12). LBR is a polytopic inner nuclear membrane protein consisting of a long, N-terminal domain, seven or eight hydrophobic transmembrane regions, and a C-terminal tail (13). The N-terminal part of the molecule protrudes to the nucleoplasm and contains multiple serine-arginine motifs that are phosphorylated by the SRPK1 and the cdc2 kinases (14, 15); the hydrophobic region represents, instead, a (functional) form of sterol reductase and is involved in cholesterol metabolism (16).

Immunodepletion of LBR from detergent-solubilized NE vesicles results in proteoliposomes with a diminished ability to bind chromatin. Furthermore, direct binding of electrophoretically purified LBR to metaphase chromosomes can be demonstrated by *in vitro* assays (17). Corroborating these observations, anti-LBR antibodies block nuclear assembly in sea urchin egg extracts (18), whereas direct (19) and indirect (20) interactions with heterochromatin protein 1 (HP1) have been claimed in the literature.

Two critical parameters in LBR-chromatin interactions are the physical state of LBR and the molecular features of LBR-associated chromatin. To address these issues, we have isolated fragments of peripheral heterochromatin attached to the inner nuclear membrane. These subcellular fractions were utilized to affinity select mononucleosomes that associate with LBR and investigate LBR-LBR interactions. The results obtained reveal specific modification "signatures" in LBR-associated histones and indicate that LBR interacts with peripheral heterochromatin as a higher oligomer.

EXPERIMENTAL PROCEDURES

Cells—Chicken and turkey erythrocytes were obtained from whole blood. HeLa cells were grown in Dulbecco's modified Eagle's medium containing 2 mM L-glutamine, 2 mM penicillin/streptomycin, and 10% fetal calf serum. Mouse fibroblasts were maintained in RPMI medium containing 2 mM L-glutamine, 2 mM penicillin/streptomycin, 10% fetal calf serum, and 50 μM 2-mercaptoethanol.

Antibodies—The characterization of anti-chicken LBR antibodies has been described previously (17, 21). Anti-mammalian LBR antibodies were produced using an antigen His-tagged N-terminal domain of human LBR. Both antibodies were affinity-purified in Affi-Gel matrices to which the N-terminal domains of chicken and human LBR were coupled. Anti-dimethylated Lys^4 and acetylated Lys^{14} histone H3 polyclonal antibodies were purchased from Upstate Biotechnology, Inc. (Lake Placid, NY). The characterization of anti-trimethylated Lys^9 histone H3 antibodies has been described (22). Affinity-purified secondary

* This work was supported by grants from the Association Francaise contre les Myopathies (France) and the General Secretariat of Research and Technology (Greece) (to S. D. G.), a core grant from the Biotechnology and Biological Sciences Research Council (United Kingdom) (to P. B. S.), a Royal Society (United Kingdom) exchange award (to P. B. S. and S. D. G.), and National Institutes of Health Grant CA20408 (to L. D. S.). The costs of publication of this article were defrayed in part by the payment of page charges. This article must therefore be hereby marked "*advertisement*" in accordance with 18 U.S.C. Section 1734 solely to indicate this fact.

§ Supported in part by a European Molecular Biology Organization short term fellowship.

§§ To whom correspondence should be addressed: Laboratory of Biology, University of Ioannina, School of Medicine, Dorouti, 45 110 Ioannina, Greece. Tel.: 30-26510-97-565; E-mail: sgeorgat@cc.uoi.gr.

[1] The abbreviations used are: NE, nuclear envelope; HP1, heterochromatin protein 1; DTT, dithiothreitol; PMSF, phenylmethylsulfonyl fluoride; NG, nuclear ghost; GST, glutathione *S*-transferase; LBR, lamin B receptor; NEPH, nuclear envelope peripheral heterochromatin fraction.

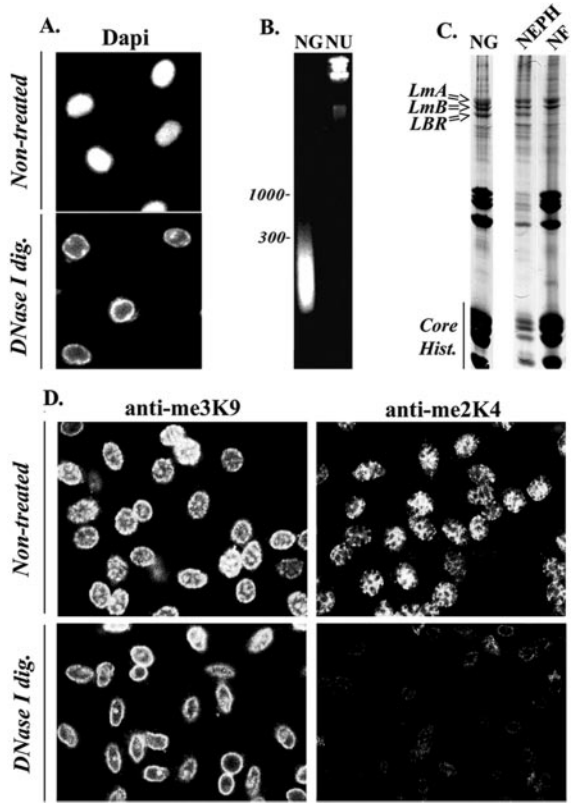

FIG. 1. **Subcellular fractionation.** *A*, images of intact (*Non-treated*) and DNase I-digested (*DNase I dig.*) avian erythrocyte nuclei after staining with 4′,6-diamidino-2′-phenylindole-dihydrochrolide (*Dapi*). *B*, electrophoretic profile of DNA extracted from nuclear ghosts (*NG*) and intact nuclei (*NU*). The positions of the 300- and 1000-bp markers are indicated. *C*, SDS-PAGE profiles of different nuclear fractions. *NEPH*, nuclear envelope vesicles and associated heterochromatin collecting at the 30–50% sucrose interface after flotation in sucrose density gradients; *NF*, nonfloating material remaining in the loading zone. Nuclear lamins (*LmA* and *LmB*), *LBR* and core histones (*Core Hist.*) are indicated. *D*, images of intact (*Non-treated*) and DNase I-digested (*DNase I dig.*) ghosts after immunostaining with anti-histone H3 antibodies. *Panel anti-me3K9*, antibodies against trimethylated Lys[9]; *panel anti-me2K4*, antibodies against dimethylated Lys[4].

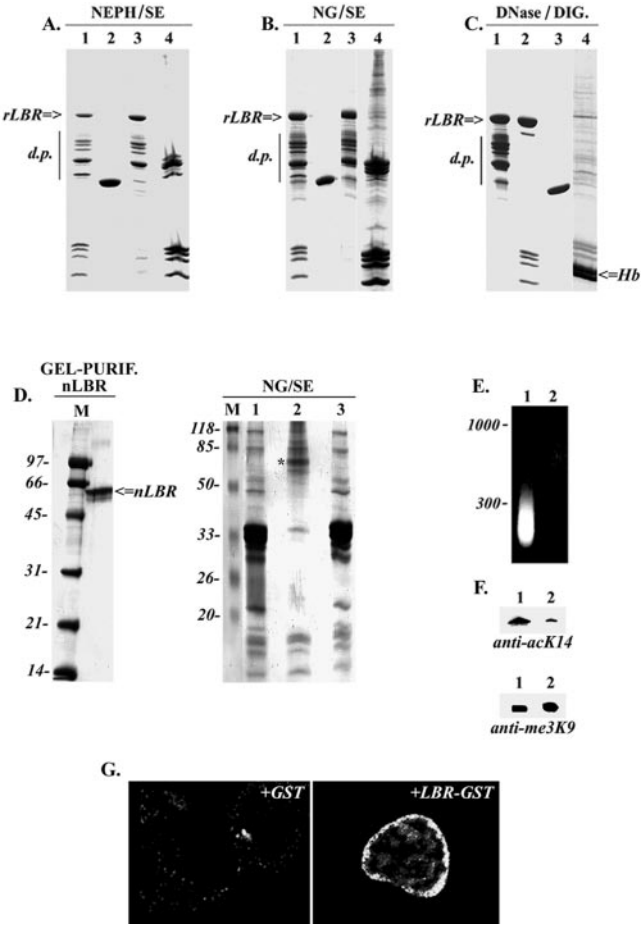

FIG. 2. **LBR binding to peripheral heterochromatin.** *A*, material precipitated by recombinant LBR-GST from salt extracts (*SE*) of floated NEPHs. *Lane 1*, proteins co-sedimenting with LBR-GST; *lane 2*, GST control; *lane 3*, input LBR-GST; *lane 4*, portion (10%) of input extract. A Coomassie Blue-stained gel is shown. *B*, same as in *A* using SEs of sonicated NGs. *C*, same as in *A* using as an input the chromatin fraction released from intact nuclei by DNase I treatment (euchromatic fraction). *Lane 1*, proteins co-sedimenting with LBR-GST; *lane 2*, proteins co-sedimenting with recombinant HP1 (M31-GST; positive control); *lane 3*, proteins co-sedimenting with GST (negative control); *lane 4*, portion (10%) of input digest. The positions of recombinant LBR (*rLBR*) and its characteristic degradation products (*d.p.*) are indicated. *Hb* denotes residual hemoglobin chains present in the crude digest. *D*, isolation of chromatin associated with endogenous, full-length LBR by affinity chromatography. The gel on the *left* shows the profile of electrophoretically purified LBR (*nLBR*) used to construct an LBR-Affi-Gel matrix; the *right panel* depicts samples of the extract that was applied to the column (*SE*; *lane 1*), the bound fraction (*lane 2*) and the nonbound fraction (*lane 3*). An *asterisk* points to traces of nLBR "leaking" from the column during elution by hot SDS sample buffer (this is commonly seen when using this matrix). *Lanes M* correspond to markers with the indicated molecular masses. *E*, electrophoretic profile of DNA extracted from the LBR-GST precipitate (*lane 1*) and the GST control (*lane 2*). The positions of the 1000- and 300-bp markers are indicated. *F*, detection of Lys[14]-acetylated and Lys[9]-trimethylated histone H3 in LBR-precipitated chromatin, as documented by Western blotting. Equal proportions of the nonbound (*lanes 1*) and the LBR-bound (*lanes 2*) material are shown. *G*, *in situ* binding of purified GST (*+GST*) and LBR-GST (*+LBR-GST*) to permeabilized HeLa cells. The cells were stained with anti-GST antibodies and visualized in a confocal microscope.

antibodies and Alexa Fluor goat anti-rabbit and donkey anti-rat IgGs were obtained from Molecular Probes (Eugene, OR).

Cell Fractionation and Preparation of Nuclear Extracts—NEs were prepared from turkey erythrocyte nuclei, essentially as specified by Refs. 17 and 23 with slight modifications. Briefly, after three rounds of DNase I digestion (80 μg/ml in 10 mM $NaPO_4$, 2 mM $MgCl_2$, 10% sucrose, 1 mM DTT, 1 mM PMSF/protease inhibitors for 15 min at room temperature, with 200 μg/ml RNase A included in the last digestion step), the resulting nuclear ghosts (NGs) were washed in buffer I (150 mM NaCl, 20 mM Tris-HCl, pH 7.5, 250 mM sucrose, 2 mM $MgCl_2$, 0.1 mM EGTA, 1 mM DTT, 1 mM PMSF), sonicated to induce vesiculation, and stored at −80 °C. NE vesicles were further purified in flotation gradients (70, 50, 30, and 20% sucrose cushions; 100,000 × *g* for 18 h at 4 °C), collecting at the 50–30% interface. The extracts were prepared by thorough resuspension of NE vesicles or sonicated NGs in 300–600 mM NaCl, 20 mM Tris-HCl, pH 7.5, 250 mM sucrose, 2 mM $MgCl_2$, 0.1 mM EGTA, 1 mM DTT, 1 mM PMSF, protease inhibitors, plus or minus 1% Triton X-100 (buffers S and ST, respectively). After ultracentrifugation (200–350,000 × *g* for 30 min at 4 °C), the soluble extracts (SE, "just salt" extract using buffer S; STE, salt and Triton extract using buffer ST) were collected and either used immediately, or further fractionated in 5–20% sucrose density gradients (100,000 × *g* at 4 °C for 18 h). A euchromatin-enriched fraction was prepared by digesting whole nuclei with DNase I (80 μg/ml, as described above). The digest was adjusted to 300 mM NaCl and 1% Triton X-100 and centrifuged at 15,000 × *g* for 30 min at 4 °C. The soluble phase was used in pull-down assays (see below).

Expression and Purification of Recombinant Proteins—Glutathione *S*-transferase (GST), GST-fused, and His_6-tagged proteins were expressed in BL21(DE3) cells and purified from lysates according to standard procedures (24).

Microscopy—For light microscopy, the samples were fixed with 1–4% formaldehyde in phosphate-buffered saline, permeabilized with 0.2% Triton X-100, and blocked with 0.5% fish skin gelatin. DNA staining (4′,6-diamidino-2′-phenylindole-dihydrochrolide, propidium iodide) and probing with the relevant primary and secondary antibodies was performed according to Ref. 25. The specimens were visualized in a *Leica SP* confocal microscope.

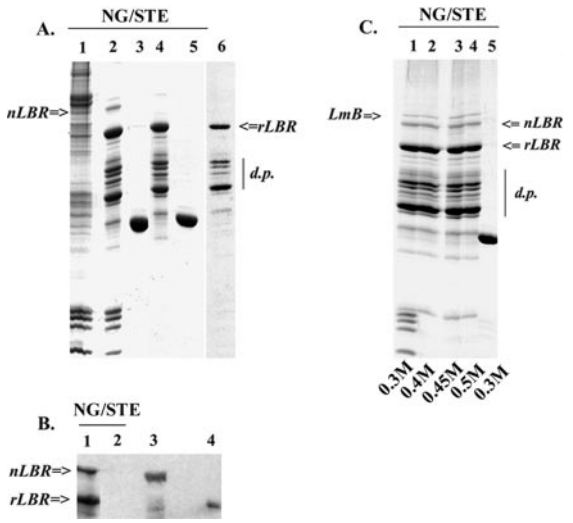

FIG. 3. **LBR self-association in STE extracts.** *A*, material precipitated by LBR-GST from STE extracts. *Lane 1*, portion (20%) of input extract; *lanes 2* and *4*, proteins co-sedimenting with LBR-GST at intermediate (0.3 M) and high (0.6 M) salt, respectively; *lanes 3* and *5*, GST controls; *lane 6*, portion (40%) of input LBR-GST. The position of LBR-GST (*rLBR*) and native (endogenous) LBR (*nLBR*) is indicated. The characteristic degradation products of LBR-GST are labeled *d.p. B*, Western blot of the material precipitated by LBR-GST (*lane 1*) and GST (*lane 2*) using affinity-purified anti-chicken LBR antibodies (only the relevant area is shown). NGs (*lane 3*) and LBR-GST (*lane 4*) have been included as standards. The designations are as in *A*. *C*, pull-down assay similar to that shown in *A*. *Lanes 1* and *5*, proteins precipitated by LBR-GST and GST, respectively, at 0.3 M salt; *lanes 2–4*, material remaining associated with LBR-GST at 0.4, 0.45, and 0.5 M NaCl. (*LmB*), traces of lamin B co-sedimenting with LBR; the other designations are as in *A*.

Pull-down Assays—GST fusion proteins (LBR-GST, M31-GST, or GST alone; 10–30 μg) were incubated first for 30 min at room temperature with 30 μl of glutathione-agarose beads in buffer S or ST (see above under "Cell Fractionation and Preparation of Nuclear Extracts"). After washing three times with the same medium, the beads were combined with nuclear extracts (SE, STE, or a DNase I digest of whole nuclei) and further incubated for 1 h at room temperature. The beads were washed five times with buffer ST and once with isotonic buffer (buffer I, see "Cell Fractionation and Preparation of Nuclear Extracts") before eluting the bound proteins with hot SDS sample buffer.

Purification of Native LBR and Affinity Chromatography in Affi-Gel Matrices—Full-length, NE-associated LBR was isolated by preparative SDS-PAGE and elution from gel pieces, essentially as described in Ref. 17. The eluted protein was reconstituted in 100 mM Hepes-NaOH, pH 7.5, 2 mM EDTA, 0.1% SDS, 2% Triton X-100, 0.2 mM PMSF, 0.05 mM DTT and dialyzed against 100 mM Hepes-NaOH, pH 7.5, 1 mM EDTA, and 0.2 mM PMSF (for 5 h at room temperature). Coupling to Affi-Gel 10/15 was done as recommended by the manufacturer (Bio-Rad). SEs were applied to the Affi-Gel-LBR column and batch-incubated for 90 min at room temperature. After thorough washing with buffer S (15 column volumes), bound material was eluted either with hot SDS sample buffer or with 1 M NaCl, 5 M urea, 40 mM Tris-HCl, pH 8.0, 1% Triton X-100, 1 mM EGTA, 1 mM DTT, and 1 mM PMSF.

Other Methods—Matrix-assisted laser desorption ionization time-of-flight mass spectrometry was performed at the Functional Genomics Unit of Moredun Research Institute (Edinburgh, UK). Protein bands were digested with R-specific protease. ΔM (the difference between the measured and calculated masses) was at the level of 1/10,000. Peak assignment was done either manually or using appropriate *Expasy* programs. Ambiguous peaks (*e.g.* those detected in histones precipitated by recombinant or endogenous LBR but not with the complex of recombinant and endogenous protein) were not taken into account. SDS-PAGE, Western blotting, and column chromatography were practiced according to established procedures.

TABLE I
Histone modifications as detected by mass spectrometry

Peak	a/a	Modifications	Bulk[a]	Extr	N + R	N	R	Modified residue
Histone H3								
704.4	3–8	nm	+	+	+	ND	+	Lys^{4}
718.4		me	+	−	−	−	−	
732.4		2×me	+F	−	−	−	−	
746.4		3×me	NR	−	−	−	−	
901.5	9–17	nm	+	+	+	+	+	Lys^{9}, Lys^{14}
943.5		3×me (ac)	+	+	+	+	+	
n.5		3×me + 2×me (ac + 2×me)	+	+	+	+	+	
985.5		3×me + 3×me (ac + 3×me)	+	+	+	+	+	
986.6	18–26	nm	NR	−	−	−	−	Lys^{18}, Lys^{23}
1028.6		ac	+	+	+	+	+	
1070.6		2×ac	+	−	−	−	−	
1433.8	27–40	nm	+	−	−	−	−	Lys^{27}, Lys^{36}
.8		3×me + me	+	+	+	++		
1250.7	54–63	nm	+	+	+	+	+	Lys^{51}
788.8	64–69	nm	+	+	+	+	+	Lys^{64}
1335.6	73–83	nm	+	+	+	+	+	Lys^{79}
n.6		2×me	+	+	+	ND	+	
1384.8	117–128	nm	+	+	+	+	+	Lys^{122}
Histone H4								
1270.8	4–17	nm	+	+	+	ND	+	Lys^{5}, Lys^{8}, Lys^{12}, Lys^{16}
8		1×ac	+	−	−	−	−	
r.8		2×ac	+	+	+	+	+	
.8		3×ac	+	+	+	ND	+	
515.3	20–23	nm	+	+	−	−	−	Lys^{20}
t.3		1×me	+	−	−	−	−	
543.3/ 855.5		2×me	+	+	+	+	+	
h.3		3×me	+	−	−	−	−	
1325.7	24–35	nm	+	+	+	+	+	Lys^{31}
1386.8	56–67	nm	+	+	+	+	+	Lys^{59}
1290.6	68–78	nm	+	+	+	+	+	Lys^{77}
1594.9	79–92	nm	+	+	+	+	+	Lys^{79}, Lys^{91}

[a] Bulk, as reported by Zhang *et al.* (30). NR, not reported; ND, not detected; F, detected by indirect immunofluoresence; a/a, amino acid position; Extra, extract of NE: N + R, native and recombinant LBR; N, native LBR; R, recombinant LBR; nm, nonmodified; ac, acetylated; me, methylated.

RESULTS

LBR Associates with Peripheral Heterochromatin—Subnuclear fractions highly enriched in peripheral heterochromatin were isolated from avian erythrocytes. Intact nuclei were extensively digested with DNase I and RNase A, yielding NGs. Consistent with previous observations (26, 27), NGs were devoid of nuclear content and retained only a layer of peripheral heterochromatin (Fig. 1*A*).[2] This "residual" chromatin was cut at multiple sites by DNase I and represented mononucleosomal particles with variable portions of linker DNA (see *broad band* at 150–200 bp in Fig. 1*B*). As could be expected (8), NE-associated chromatin was essentially depleted of Lys^4-dimethylated histone H3 but possessed Lys^9-trimethylated histone H3 (Fig. 1*D*).

On a mg/mg basis, NGs contained significantly more histones than NE proteins (*e.g.* lamins and LBR; Fig. 1*C*). However, upon further fractionation in sucrose flotation gradients, loosely attaching chromatin dissociated from the inner nuclear membrane and the material collecting at the 30–50% interface (nuclear envelope-peripheral heterochromatin fraction (NEPH)) possessed almost stoichiometric amounts of histones and NE proteins (Fig. 1*C*).

To examine whether LBR associates with a specific fraction of chromatin, we performed pull-down experiments using exogenous (recombinant) LBR. As shown in Fig. 2 (*A*, *B*, and *E*), a GST fusion protein corresponding to the N-terminal domain of LBR precipitated roughly stoichiometric amounts of heterochromatin-derived core particles obtained from NG and NEPH salt extracts. However, unlike recombinant HP1 (M31), recombinant LBR did not precipitate nucleosomes when NEPH extracts were substituted with euchromatin-enriched DNase I digests of whole nuclei (Fig. 2*C*). The binding of HP1 to particles released by DNase I digestion is consistent with recent observations that reveal a role of this protein in the organization of both hetero- and euchromatin (28). On the other hand, the selective association of LBR with nucleosomes that co-fractionate with the NE indicates a preference for peripheral heterochromatin. Consistent with this idea, when permeabilized HeLa cells were incubated with recombinant LBR, the nuclear periphery was intensely decorated, whereas under the same conditions, the staining of internal nuclear sites was rather faint (Fig. 2*G*).

As expected from previous studies (17), native (endogenous) LBR purified by preparative electrophoresis and coupled to Affi-Gel also "selected" a fraction of nucleosomes contained in SEs (Fig. 2*D*, *lanes 2* and *3*). This enabled comparisons of the chemical modifications in histones H3/H4 associated with either the native or the recombinant protein (see below).

Modification Signatures of NE/LBR-associated Chromatin—To characterize the LBR-associated chromatin fraction, we excised the histone H3/H4 bands from SDS gels (similar to those shown in Fig. 2, *A*, *B*, and *D*) and subjected the samples to mass spectrometry (matrix-assisted laser desorption ionization time-of-flight MS). To be more systematic, we also analyzed histones co-precipitating with a complex of recombinant and endogenous LBR (for details see Fig. 3*A*). As shown in Table I, nucleosomes affinity-selected by LBR and nucleosomes extracted from NEs yielded almost the same histone H3/H4 modification signatures. Some of the peaks detected in the histones that co-precipitated with recombinant or a complex of endogenous and recombinant LBR were not detected in the samples eluted from Affi-Gel columns containing exclusively

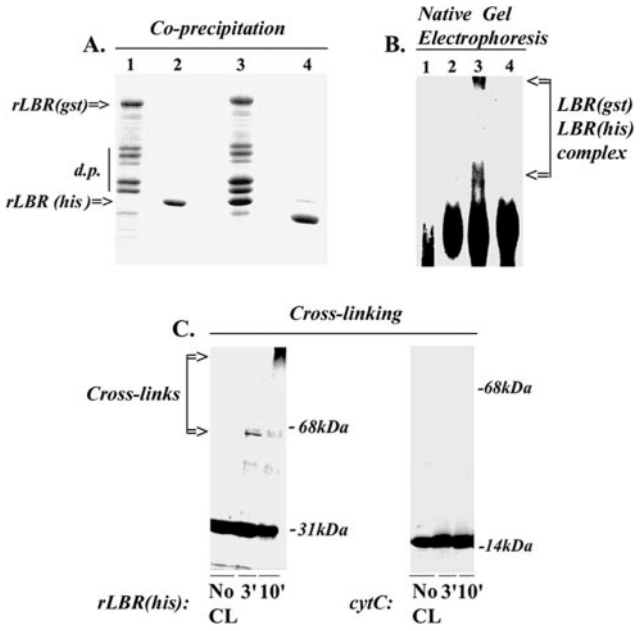

FIG. 4. **LBR oligomerization.** *A*, co-precipitation of purified LBR-GST and LBR-His_6. *Lane 1*, input LBR-GST; *lane 2*, input LBR-His_6; *lane 3*, material precipitated by LBR-GST; *lane 4*, GST control. *B*, detection of LBR-LBR complexes by native gel electrophoresis. *Lane 1*, input LBR-GST; *lane 2*, input LBR-His_6; *lane 3*, LBR-GST and LBR-His_6; *lane 4*, LBR-His_6 and GST. The bands appearing only in the mixture of LBR-GST and LBR-His_6 are indicated by *arrows*. *C*, cross-linking experiments. The *two panels* show SDS gels stained with Coomassie Blue. *No CL*, is the non-cross-linked material; samples (*3′*) and (*10′*) depict cross-linking products after 3- and 10-min incubations with 0.03% glutaraldehyde. An assay with LBR-His_6 is depicted on the *left*, whereas the corresponding control with cytochrome *c* is shown on the *right*. The migration of molecular weight markers with the indicated molecular masses is denoted.

endogenous LBR. However, these differences were minor and did not alter the overall picture emerging from the mass spectrometric data (for instance, most of the missing peaks corresponded to either nonmodified or partially modified peptides and not to fully modified ones).

LBR or NE-associated particles exhibited features that clearly differentiated them from bulk chromatin (29–31). First, Lys^4 of histone H3 was not modified, consistent with the indirect immunofluorescence data presented in Fig. 1*D*; second, although histone H3 monoacetylated in Lys^{18} or Lys^{23} could be readily identified, species acetylated in both residues were not detected. This was observed with several different preparations and did not change when the chromatin fractions were isolated in the presence of sodium butyrate.

In LBR-associated nucleosomes, the histone fold domain of H3 and H4 was largely nonmodified (with the exception of Lys^{79} in histone H3). Lys^{27} and Lys^{36} of H3 were modified by trimethylation, whereas H4 was dimethylated in Lys^{20} and partially or fully acetylated at Lys^5, Lys^8, Lys^{12}, and Lys^{16}. Histone H3 was heavily modified in the region 9–17, which contains Lys^9 and Lys^{14}. Because the mass difference corresponding to lysine trimethylation is equal to that of lysine acetylation, a peak at 971.5 daltons could be assigned either to a dimethylated/acetylated or to a dimethylated/trimethylated 9–17 peptide. Likewise, another peak at 985.5 could be attributed either to a twice trimethylated or to a trimethylated/acetylated peptide. Pull-down assays with recombinant LBR and Western blotting with anti-histone modification antibodies showed that H3 subspecies trimethylated at Lys^9 or acetylated Lys^{14} were present in the LBR precipitate, albeit to a different extent (Fig. 2*F*). Although this does not prove that LBR-associated nucleosomes contain histone H3 that is *simultaneously*

[2] D. Makatsori, N. Kourmouli, H. Polioudaki, L. D. Shultz, K. Mclean, P. A. Theodoropoulos, P. B. Singh, and S. D. Georgatos, unpublished data.

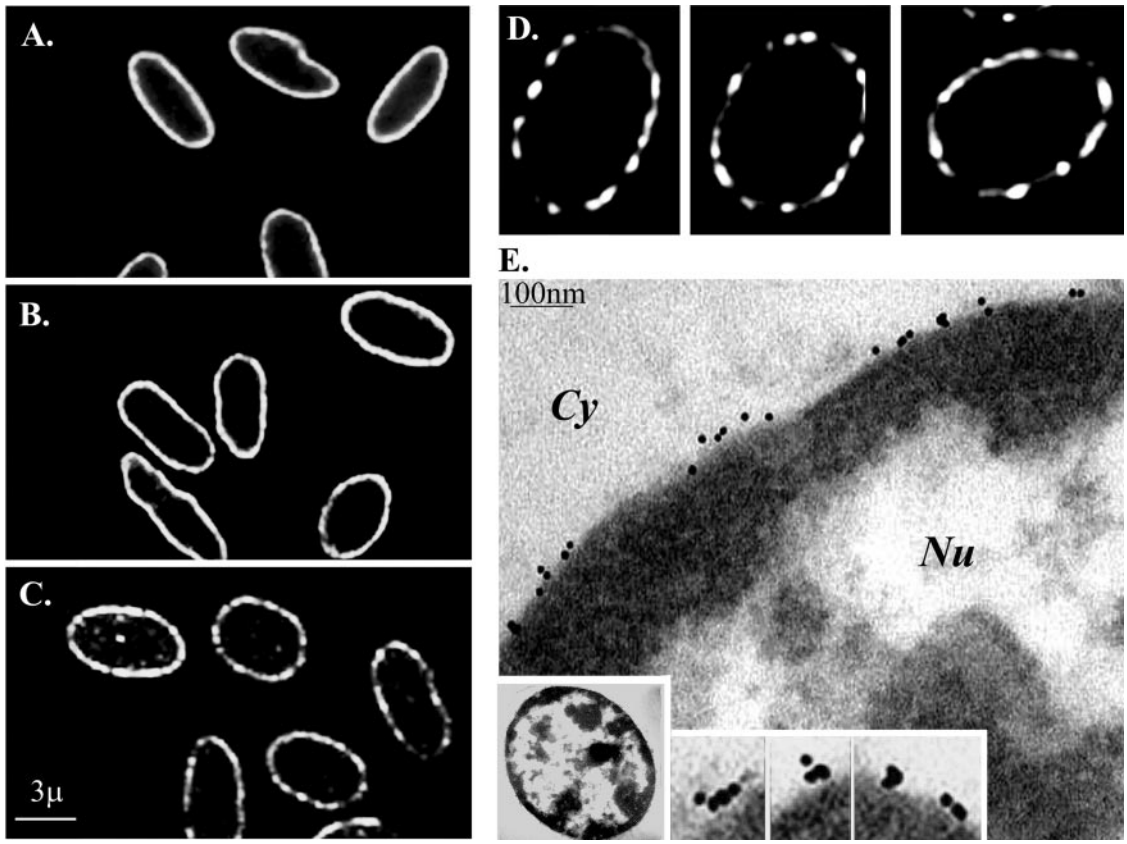

FIG. 5. ***In situ* organization of LBR in avian erythrocytes.** Specimens decorated with anti-lamin A (*A*), anti-lamin B (*B*), and anti-chicken LBR (*C*) antibodies, as visualized in the confocal microscope. *D* shows representative LBR profiles at higher contrast and magnification. All of the images represent nearly equatorial optical sections. *E*, part of an erythrocyte nucleus, as visualized after pre-embedding immunoelectron microscopy with affinity-purified anti-chicken LBR antibodies and protein A-gold. The *insets* at the *bottom* show a low power view of the entire nucleus (*left inset*) and a series of electron microscopy images with clusters of immunogold particles (*three right insets*). *Cy*, cytoplasm; *Nu*, nucleus. Magnification is indicated by *bars*.

modified at Lys^9 and Lys^{14}, it can be safely concluded that acetylation in Lys^{14} is not incompatible with heterochromatin association and LBR binding.

LBR Self-associates under in Vitro Conditions—When salt/detergent extracts (STE) were used in the pull-down experiments instead of just salt SEs, we noticed that recombinant LBR consistently precipitated a protein co-migrating with endogenous, full-length LBR and traces of nuclear lamin B (Fig. 3*A*). The presence of endogenous LBR in the LBR-GST precipitate could be confirmed by Western blotting (Fig. 3*B*) and explained either by "cross-linking" through nucleosomes/lamin B and/or direct LBR-LBR binding (oligomerization). To distinguish between these possibilities, we performed the pull-down assay at 0.3 M salt and subsequently washed the precipitates with increasing NaCl concentrations (notice that co-precipitation of native LBR and nucleosomes with recombinant LBR is abolished at 0.6 M NaCl; Fig. 3*A*). As illustrated in Fig. 3*C*, native LBR was retained in the LBR-GST precipitate after washing with 0.4, 0.45, or 0.5 M salt, when all of the nucleosomes had detached. Furthermore, direct evidence for *in vitro* oligomerization was obtained using GST-tagged and His_6-tagged LBR. As shown in Fig. 4*A*, the two forms of recombinant LBR co-precipitated. In addition, LBR-GST/LBR-His_6 complexes were readily detectable in nondenaturing acrylamide gels (Fig. 4*B*). Finally, LBR-His_6 could be cross-linked by glutaraldehyde, yielding dimers and higher order oligomers. Under the same conditions, a control protein of analogous charge and molecular mass (cytochrome *c*) was not cross-linked (Fig. 4*C*).

LBR Resides in Distinct NE Microdomains—That the N-terminal domain of LBR oligomerized *in vitro* suggested that the native protein might form microdomains at the level of the NE. To explore this idea, we proceeded with morphological experiments. A striking, "lumpy" fluorescence pattern was observed when avian erythrocytes were decorated by chicken LBR-specific, affinity-purified antibodies and examined by confocal microscopy (Fig. 5, *C* and *D*). This discontinuous pattern contrasted the smooth, uniform staining of the nuclear periphery with anti-lamin A and anti-lamin B antibodies (Fig. 5, *A* and *B*) and was apparent at both *xy* and *xz* optical sections (see below). Discrete LBR "islets" could also be discerned when Triton-permeabilized erythrocytes were examined by pre-embedding immunoelectron microscopy (Fig. 5*E*).

Heterozygous Mutations Affect LBR Organization and Nuclear Structure—To study in more detail LBR organization *in vivo*, we examined fibroblasts from wild type and ichthyosis (*ic*) mouse mutants. Some of these mutations (ic^J) result in a frame shift that changes amino acids 365–385 and introduces a stop codon at residue 386 of the LBR gene. Homozygous animals do not contain immunohistochemically identifiable LBR in the inner nuclear membrane (32), because, most likely, the mutant protein is degraded shortly after synthesis on ER membranes. However, we reasoned that heterozygous *ic* mutants might be informative; because the truncated *ic*-LBR has an intact N-terminal domain, oligomerization with wild type LBR may rescue some of this protein and produce an intermediate, analyzable phenotype.

Staining of wild type fibroblasts with affinity-purified, anti-mammalian LBR-specific antibodies revealed that the intact protein is localized in NE microdomains, very much like its avian counterpart (Fig. 6, *wild type*, *A–D*). The LBR islets were

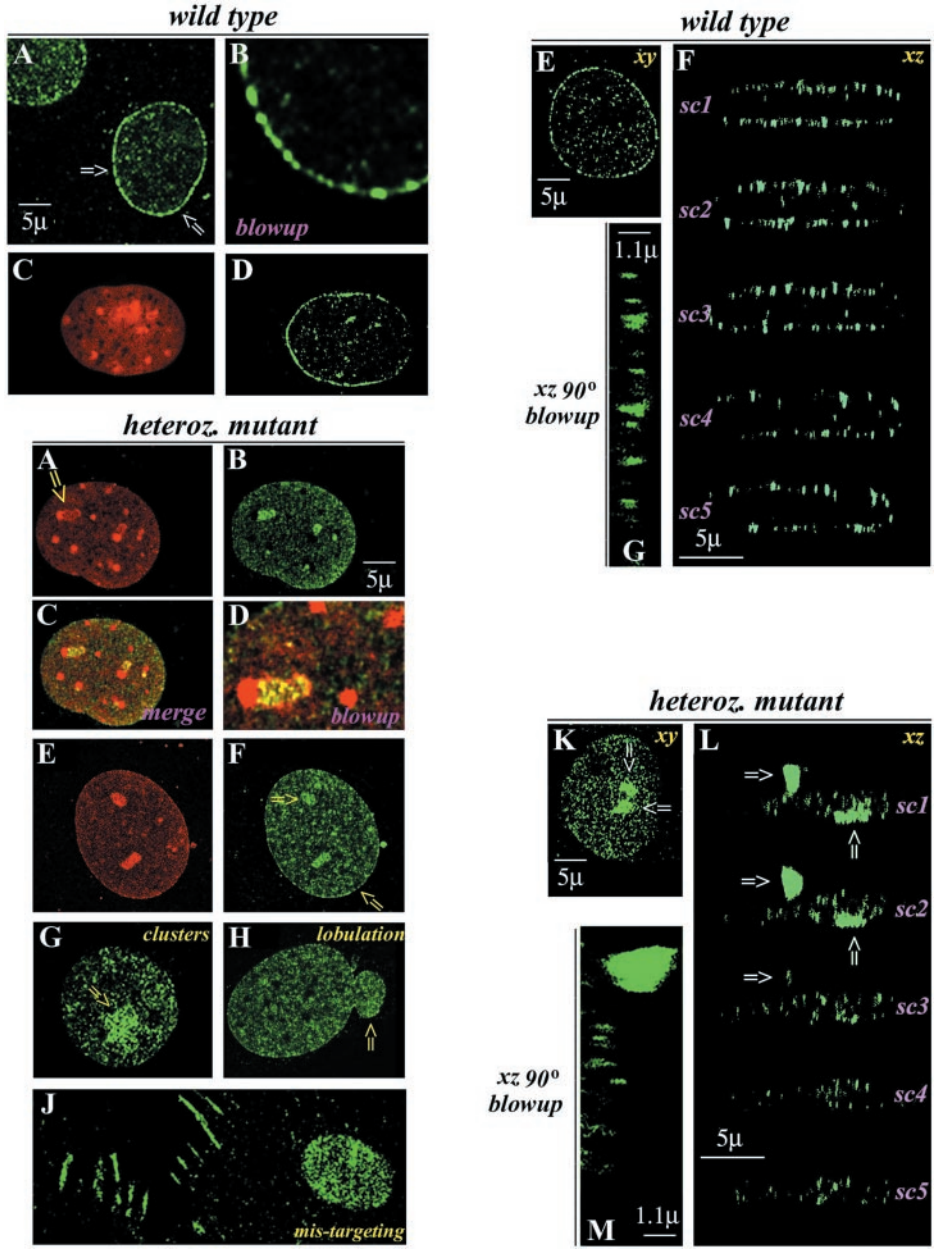

FIG. 6. ***In situ* organization of LBR in mouse fibroblasts.** *A*, *B*, and *D–G* show staining of wild type cells with affinity-purified, anti-mammalian LBR antibodies. A 3× blowup of the area marked by *arrows* in *A* is shown in *B*. *C* represents a propidium iodide profile of the same cell depicted in *D*. *F* shows a series of *xz* sections (*sc1–5*) of the cell that is imaged at the *xy* level in *E*. *G* is a 90-degree rotated blowup of a part of *sc2*, for a better appreciation of the size and regularity of LBR microdomains. *B* and *F–M* show staining of heterozygous *ic* mutant cells with anti-LBR antibodies. *A* is a propidium iodide profile of the same cell shown in *B*. *C* and *D* are fluorescein isothiocyanate/propidium iodide merges of *A* and *B* at relative magnifications of 1× and 3-, respectively. The spatial relationship of heterochromatin foci and LBR clusters (*arrow* in *A*) is apparent in the 3× blowup. *E* is the same cell depicted in *F*, counter-stained with anti-lamin A/C antibodies; a surface LBR aggregate, and a segment of the NE exhibiting normal rim fluorescence in this doubly stained specimen are indicated (*arrows*). *G–J* depict various abnormalities observed in mutant cells (large LBR *clusters* on the surface of the nucleus, nuclear *lobulation*, and *mis-targeting* of LBR to adhesion plaques). *K–M* represent *xy*/*xz* series, as described above for wild type cells. Two large LBR clusters, one in a vertical "outgrowth" of the NE and the other on the basal surface of the nucleus, are indicated by *arrows*. The *bars* in each group of images indicate magnification.

of considerable size (500–800 nm) and in *xz* sections produced a striking "palisade" pattern along the nuclear periphery (*panels E–G*). In heterozygotic cells, the rim fluorescence pattern was not immediately obvious; instead, in 50% of the cells LBR appeared to form large nucleoplasmic "blocks" that superficially resembled foci of pericentric heterochromatin or nucleoli (Fig. 6, *heteroz. mutant*, *B* and *G*). Upon closer inspection, it became clear that these LBR aggregates were adjacent to but not coincident with internal heterochromatic foci (Fig. 6, *A–D*). Furthermore, double staining with anti-LBR/anti-lamin antibodies (Fig. 6, *E* and *F*) and confocal series along the *xz* axis (Fig. 6, *K–M*) revealed that these blocks, which replace the more or less evenly distributed LBR microdomains, represented large patches of NE-associated material.

As expected, besides the effects on the subnuclear distribution of LBR, some of the mutant cells exhibited gross sorting defects, with a fraction of LBR ending up in adhesion plaques (Fig. 6*J*, *mis-targeting*; ~60% of the cells). Finally, consistent with the critical role of LBR in nuclear reassembly and architecture (17), some of the mutant cells, often in groups, appeared to have irregularly shaped nuclei (Fig. 6*H*, *lobulation*; ~30% of the cells). Taken together, these results reinforce the idea that LBR self-associates via its N-terminal domain and forms distinct microdomains *in vivo*. Apparently, the fine structure of these assemblies is greatly affected in *ic* cells, in which the protein encoded by the altered allele behaves as a dominant-negative mutant.

DISCUSSION

Features and Epigenetic Marks of LBR-associated Chromatin—To isolate peripheral heterochromatin, we have taken advantage of previous observations (26, 27) showing that the central "core" of chromatin is effectively removed from the avian erythrocyte nucleus upon DNase I digestion. The choice of nuclease seems to be critical; in comparative experiments we have found that micrococcal nuclease is less efficient than DNase I and, depending on the conditions, yields variable results.

The NGs obtained after DNase I digestion were found to contain a more or less intact NE, underlined by a layer of peripheral heterochromatin. With controlled sonication, these "shells" are converted to small vesicles that have an inside-out

orientation (17, 27)[2] and can be further fractionated by flotation in sucrose density gradients (NEPH fraction).

We have shown here that mononucleosomes extracted from NEPHs and NGs bind almost stoichiometrically to LBR. Mass spectrometric analysis indicates that LBR-associated particles contain histone H3 that is methylated at Lys^{9} and Lys^{27}, monoacetylated in Lys^{18} and Lys^{23}, and nonmodified at all at Lys^{4}. The same type of analysis reveals more complicated patterns of post-translational modification, such as trimethylation of Lys^{9} combined with acetylation (or, less likely, trimethylation) at Lys^{14} (histone H3) and partial acetylation of Lys^{5}, Lys^{8}, Lys^{12}, and Lys^{16} (histone H4). Some of these combinations, which clearly occur in native heterochromatin, would not be anticipated from the currently established rules of the "histone code" (8).

Because *in vitro* acetylation of purified histones H3/H4 by CREB-CBP reduces significantly *in vitro* binding to LBR (20), nucleosomes containing such acetylated species are not expected to associate directly with the inner nuclear membrane. However, as we argued previously (20), the binding properties of purified histones or histone tail peptides might be different from that of native nucleosomes; sites "occluded" or buried in the fully assembled particle could be partially exposed when histones are dissociated from one another. In addition, long range interactions between different "modification cassettes" (9) may not occur when histone peptides are used instead of the intact H3/H4.

It is theoretically possible that nucleosomes containing partially acetylated histones associate with LBR through "bridging" particles, which consist of nonacetylated histones and are laterally connected to the former via nucleosome-nucleosome interactions. However, this possibility is remote, because the preparations used in this study contained *mono*nucleosomes, whereas binding of core particles to LBR was almost stoichiometric (nonstoichiometric binding should be expected if LBR associates with arrays of polynucleosomes instead of mononucleosomes).

LBR Self-association and NE Microdomains—Accumulating evidence suggests that several integral proteins of the NE (*e.g.* LAP1, LAP2, and LBR) are organized as multi-subunit complexes and may form chromatin-remodeling platforms. In rat hepatocytes, LAP1 localizes in regularly spaced clusters and is co-immunoprecipitated with B-type lamins and a calcium-dependent kinase (33). Along similar lines, LAP2B can be cross-linked and co-precipitated with at least four other nuclear proteins, including LBR and HA95 (34). LBR is also co-isolated from avian erythrocytes together with the nuclear lamins, an SR kinase (SRPK1), a splicing factor-associated element (p32/p34), and a membrane protein related to peripheral benzodiazepine receptors (35, 36). Finally, LBR binding to HP1 (19), or a HP1-core histone subcomplex (20), occurs under certain conditions.

At this point, it is not clear whether inner nuclear membrane proteins participate in the formation of these complexes as individual monomers or as higher oligomers. Using *in vitro* assays, we have demonstrated that (at least) LBR self-associates through its N-terminal domain and forms specific oligomers under stringent ionic conditions (*i.e.* at 0.15–0.5 M salt). Furthermore, employing two different affinity-purified antibodies and a range of morphological techniques, we have shown that native LBR resides in distinct NE microdomains. From the morphological analysis of heterozygous LBR mutants, it looks likely that the normal distribution and fine substructure of LBR microdomains are affected significantly in pathological conditions, such as ichthyosis or the Pelger-Huet anomaly (32). Therefore, heterozygous animals provide an excellent model system for further analysis of LBR-LBR and LBR-chromatin interactions.

Because native heterochromatin contains arrays of tandemly repeated elements (*e.g.* nucleosome chains with specifically modified histone tails), it is perhaps not surprising that its NE anchor, LBR, may also exist in the form of a multimeric particles. Nonetheless, one idea that needs to be investigated further is whether the hydrophobic domain of LBR, in its capacity as a sterol reductase (16), modifies the local lipid environment and supports the formation of specific LBR "rafts." So far, attempts to isolate such proteolipid assemblies by flotation in sucrose gradients have not been successful. However, this task might be more complicated than it seems, because the composition of LBR-associated lipids and the stability of the putative rafts to different detergents have not yet been systematically explored.

Acknowledgments—We are grateful to G. Griffiths (EMBL) for providing facilities and advice on electron microscopy and A. S. Politou, S. Christoforidis (University of Ioannina, Ioannina, Greece), and C. Murphy (Foundation for Research and Technology-Biomedical Research Institute of Ioannina (FORTH-BRI), Ioannina, Greece) for materials. We acknowledge Bruce Gott, Charlie Lerner, and Lisa Burzenski for their technical support. Finally, we acknowledge P. Kouklis for thoroughly reading the manuscript.

REFERENCES

1. Carvalho, C., Pereira, H. M., Ferreira, J., Pina, C., Mendonca, D., Rosa, A. C., and Carmo-Fonseca, M. (2001) *Mol. Biol. Cell* **12,** 3563–3572
2. Bridger, J. M., and Bickmore, W. A. (1998) *Trends Genet.* **14,** 403–409
3. Bridger, J. M., Boyle, S., Kill, I. R., and Bickmore, W. A. (2000) *Curr. Biol.* **10,** 149–152
4. Lamond, A. I., and Earnshaw, W. C. (1998) *Science* **280,** 547–553
5. Tumbar, T., and Belmont, A. S. (2001) *Nat. Cell Biol.* **3,** 134–139
6. Georgatos, S. D. (2001) *EMBO J.* **20,** 2989–2994
7. Foisner, R. (2001) *J. Cell Sci.* **114,** 3791–3792
8. Fischle, W., Wang, Y., and Allis, C. D. (2003) *Curr. Opin. Cell Biol.* **15,** 172–183
9. Fischle, W., Wang, Y., and Allis, C. D. (2003b) *Nature* **425,** 475–479
10. Spector, D. L., and Gasser, S. M. (2003) *EMBO Rep.* **4**, 18–23
11. Andrulis, E. D., Neiman, A. M., Zappulla, D. C., and Sternglanz, R. (1998) *Nature* **394,** 592–595
12. Worman, H. J., Yuan, J., Blobel, G., and Georgatos, S. D. (1988) *Proc. Natl. Acad. Sci.* **85,** 8531–8534
13. Worman, H. J., Evans, C. D., and Blobel, G. (1990) *J. Cell Biol.* **111,** 1535–1542
14. Nikolakaki, E., Simos, G., Georgatos, S. D., and Giannakouros, T. (1996) *J. Biol. Chem.* **271,** 8365–8372
15. Nikolakaki, E., Meier, J., Simos, G., Georgatos, S. D., and Giannakouros, T. (1997) *J. Biol. Chem.* **272,** 6208–6213
16. Holmer, L., Pezhman, A., and Worman, H. J. (1998) *Genomics* **54,** 469–476
17. Pyrpasopoulou, A., Meier, J., Maison, C., Simos, G., and Georgatos, S. D. (1996) *EMBO J.* **15,** 7108–7119
18. Collas, P., Courvalin, J. C., and Poccia, D. (1996) *J. Cell Biol.* **135,** 1715–1725
19. Ye, Q., and Worman, H. J. (1996) *J. Biol. Chem.* **271,** 14653–14656
20. Polioudaki, H., Kourmouli, N., Drosou, V., Bakou, A., Theodoropoulos, P. A., Singh, P. B., Giannakouros, T., and Georgatos, S. D. (2001) *EMBO Rep.* **2,** 920–925
21. Meier, J., and Georgatos, S. D. (1994) *EMBO J.* **15,** 1888–1898
22. Cowell, I. G., Aucott, R., Mahadevaiah, S. K., Burgoyne, P. S., Huskisson, N., Bongiorni, S., Prantera, G., Fanti, L., Pimpinelli, S., Wu, R., Gilbert, D. M., Shi, W., Fundele, R., Morrison, H., Jeppesen, P., and Singh, P. B. (2002) *Chromosoma* **111,** 22–36
23. Georgatos, S. D., and Blobel, G. (1987) *J. Cell Biol.* **105,** 117–125
24. Sambrook, J., Fritsch, E. F., and Maniatis, T. M. (1989) *Molecular Cloning: A Laboratory Manual*, 3rd Ed., Cold Spring Harbor Laboratory Press, Cold Spring Harbor, NY
25. Maison, C., Horstmann, H., and Georgatos, S. D. (1993) *J. Cell Biol.* **123,** 1491–1505
26. Harris, J. R., and Brown, J. N. (1971) *J. Ultrastruct. Res.* **36,** 8–23
27. Harris, J. R. (1978) *Biochim. Biophys. Acta* **515,** 55–104
28. Piacentini, L., Fanti, L., Berloco, M., Perrini, B., and Pimpinelli, S. (2003) *J. Cell Biol.* **161,** 707–714
29. Zhang, K., and Tang, H. (2003) *J. Chromatogr. B. Analyt. Technol. Biomed. Life Sci.* **783,** 173–179
30. Zhang, K., Tang, H., Huang, L., Blankenship, J. W., Jones, P. R., Xiang, F., Yau, P. M., and Burlingame, A. L. (2002) *Anal. Biochem.* **306,** 259–269
31. Zhang, L., Eugeni, E. E., Parthun, M. R., and Freitas, M. A. (2003) *Chromosoma* **112,** 77–86
32. Shultz, L. D., Lyons, B. L., Burzenski, L. M., Gott, B., Samuels, R., Schweitzer, P. A., Dreger, C., Herrmann, H., Kalscheuer, V., Olins, A. L., Olins, D. E., Sperling, K., and Hoffmann, K. (2003) *Hum. Mol. Genet.* **12,** 61–69
33. Maison, C., Pyrpasopoulou, A., Theodoropoulos, P. A., and Georgatos, S. D. (1997) *EMBO J.* **15,** 4839–4850
34. Martins, S. B., Eide, T., Steen, R. L., Jahnsen, T., Skalhegg, B. S., and Collas, P. (2000) *J. Cell Sci.* **113,** 3703–3713
35. Simos, G., and Georgatos, S. D. (1992) *EMBO J.* **11,** 4027–4036
36. Simos, G., Maison, C., and Georgatos, S. D. (1996) *J. Biol. Chem.* **24,** 12617–12625